Considerations on Hund's first rule in a planar two-electron quantum dot

Sebastian Schröter,[1] Harald Friedrich,[1] and Javier Madroñero[1,2]
[1]*Physik Department, TU München, D-85747 Garching, Germany*
[2]*Departamento de Física, Universidad del Valle, Cali, Colombia*
(Received 28 February 2013; published 12 April 2013)

We give a detailed analysis of the applicability of Hund's first rule for harmonic planar two-electron quantum dots by means of entanglement witnesses. We find that for purely harmonic confinement there is only one pair of singlet and triplet states for which it can be applied. We also discuss the origin and validity for this case and extend the discussion to a quartic confining potential, a hard-wall potential, and a combination of harmonic confinement with quartic perturbation. A generalized rule, the *alternating rule*, is found to be applicable and valid for vanishing angular momentum states in all these cases. Furthermore, we are able to clarify the role of entanglement in general harmonic two-electron models for vanishing interaction strength. This behavior can be attributed to the special separability properties of these models.

DOI: 10.1103/PhysRevA.87.042507 PACS number(s): 31.10.+z, 03.67.Mn, 31.15.A−, 73.21.La

I. INTRODUCTION

Hund's first rule (HFR) [1,2] is well known to have universal predictive power for the ground-state electron configuration of atoms. In case of equal spatial configuration the higher spin state has less energy than the lower spin state. The rule can be generalized to excited states with the same configuration of one-electron orbitals [3].

There has been a long discussion about the origin of this effect, starting from the first explanation by Slater [4]. He claimed that the difference in Coulomb interaction between the electrons due to the existence of a Fermi hole was responsible for this effect. More than 30 years later a numerical calculation by Davidson [5] for helium was the first to reveal that Slater's argumentation was wrong; in fact the Coulomb interaction was higher for the triplet state. Several calculations for helium and heliumlike ions supported this result [6–9]. Calculations for atomic systems with more electrons, e.g., Ref. [10], confirmed this behavior. A result based on perturbation theory [11,12] showed that generally all atoms violate Slater's explanation and a new interpretation was given by Boyd [13]. His argumentation follows the virial theorem for atomic systems: The total energy equals half of the potential energy. All interactions are Coulombic and the potential energy is the sum of the interelectron and the negative electron-nucleus interactions. As a consequence the absolute value of the nuclear potential energy must rise for higher spin states to compensate the higher interelectron interaction. This could be interpreted as a higher effective nuclear charge or lower screening of the nuclear attraction, caused by different angular configurations. Only recently this interpretation has again been doubted by Sajeev *et al.* [14] when they compared the effect in atoms to rectangular quantum dots. They claim that the angular configuration does not play a major role for screening effects. A detailed review of the meaning and applicability of Hund's rules can be found in [15]. A generalization of HFR, the *alternating rule*, was first proposed by Morgan and Kutzelnigg [3] distinguishing different behaviors between natural and unnatural parity states. The comparison of the results for heliumlike systems with harmonic quantum dot systems has been addressed recently by Sako *et al.* [16], and also by Katriel *et al.* [17]. Just like in atoms, the filling of the electron orbitals for few-electron quantum dots in the ground state is in general governed by Hund's rules [18–20].

In the present paper, we address the applicability, the range of validity, and the origin of HFR in the widely used planar harmonic confinement model for two-electron quantum dots. In addition, we investigate the same issues for the *alternating rule* [3]. This rule is shown to be applicable and extensively valid for zero-angular-momentum states in a planar two-electron model with quartic confinement, and also for harmonic confinement with quartic deviation.

The interparticle interaction is the driving force for the energy splitting between singlet and triplet states. Appropriate quantum numbers and probability densities obtained in center-of-mass (COM) and relative coordinates reveal the importance of the interparticle potential. This enables us to give an interpretation that holds not only for HFR, but also for the *alternating rule*, for both the harmonic and the quartic potentials.

The planar harmonic model has already been addressed in [16,21], and we agree with the main conclusion, that the cause of the lower energy for the triplet state is the angular momentum configuration in the relative motion. However, only very little attention has been paid to a detailed investigation of the applicability of Hund's rules. We find evidence that there is only one pair of states of each parity, even and odd, for which HFR is applicable at all.

We investigate measures for the entanglement between two fermions [22], in order to obtain an explicit quantity bearing the information on applicability of HFR. These measures of the entanglement are calculated analytically in the noninteracting limit. We only presume the system to be in the symmetry class appropriate for the interaction depending on the interelectron distance. Our results are therefore applicable not only to Hooke's atom with Coulomb interaction, but also to Crandall's atom, with inverse square interaction and Moshinsky's atom with harmonic interaction. The entanglement of these and similar models have been considered recently [23,24] and the entanglement of several excited states has been found to be nonvanishing in the noninteracting limit, which might seem counterintuitive. Another issue has been discussed when comparing these results to the conceptually similar system of helium, which has Coulombic confinement [24–26]. The

linear entropy for the harmonic models was found to saturate to unity, while for helium the limit is one-half. Both effects can be clarified by our analysis of the entanglement.

In Sec. II we briefly describe our model for a planar quantum dot which has been presented in detail in [27]. A general discussion about entanglement and separability of the system is presented in Sec. III. Section IV is devoted to the discussion of the applicability of HFR in the case of harmonic confinement. In Sec. V we address the quartic confinement and show our results supporting the *alternating rule*. Before we conclude in Sec. VII, we briefly discuss the *alternating rule* in a combination of a harmonic with a weak quartic potential and also in a planar hard-wall quantum dot model in Sec. VI.

II. GENERAL MODEL

We discuss a planar model of two electrons confined by a harmonic or quartic potential interacting via Coulomb interaction. The Hamiltonian in modified units (m.u.) (see Appendix A) reads

$$H = \sum_{j=1}^{2}\left[-\frac{1}{2}\nabla_j^2 + V_{\text{conf}}(\boldsymbol{r}_j)\right] + \frac{\gamma}{|\boldsymbol{r}_1 - \boldsymbol{r}_2|}. \tag{1}$$

Here the adiabatic introduction of the interparticle interaction can be tuned by the Coulomb strength parameter γ and the confining potential is defined by one of

$$V_{\text{harmonic}}(\boldsymbol{r}) = \tfrac{1}{2}\boldsymbol{r}^2, \tag{2}$$

$$V_{\text{quartic}}(\boldsymbol{r}) = (\boldsymbol{r}^2)^2. \tag{3}$$

For all cases we consider the following set of operators commuting with the Hamiltonian and each other: The square of the total angular momentum perpendicular to the plane L_z^2, the particle exchange operator Π_{12}, and the parity operator Π_{xy}, interchanging the coordinates x and y. The corresponding eigenvalues are m^2 with $|m| \in \mathbb{N}$, $\epsilon_s \in \{+1\,(\text{singlet}), -1\,(\text{triplet})\}$, and $\epsilon_p \in \{+1\,(\text{even}), -1\,(\text{odd})\}$, respectively. For details of the approach we refer to Ref. [27].

The Hamiltonian can be written as the sum of the kinetic energy, the confining potential, and the interparticle interaction potential. From the quantum virial theorem it is well known that there is an interdependence between the expectation values of these contributions in an eigenstate.

From our point of view the expectation value of the kinetic energy is to be considered as a consequence of the potentials involved and we write the eigenenergy as the weighted sum of the expectation values of the potentials:

$$E_{\text{harmonic}} = 2\,\langle V_{\text{harmonic}}\rangle + \tfrac{1}{2}\,\langle V_{\text{Coulomb}}\rangle, \tag{4}$$

$$E_{\text{quartic}} = 3\,\langle V_{\text{quartic}}\rangle + \tfrac{1}{2}\,\langle V_{\text{Coulomb}}\rangle. \tag{5}$$

Note that our numerical results agree with the virial theorem up to the full accuracy of the eigenenergies. The importance of the virial theorem and the preservation by the numerical results for an interpretation of Hund's rules has been pointed out recently by Oyamada *et al.* [28].

III. ENTANGLEMENT AND SEPARABILITY

Entanglement for indistinguishable particles, where all states are linear superpositions, has attained much interest in recent years. A clear description of the bosonic and fermionic entanglement properties has been given in [29,30]. For a fermionic state $|\Psi\rangle$ the Slater rank is introduced, which is the minimal number of nonvanishing coefficients in the Slater decomposition:

$$|\Psi\rangle = \sum_{j,k} c_{j,k}(|\psi_{1,j}\rangle \otimes |\psi_{2,k}\rangle - |\psi_{2,j}\rangle \otimes |\psi_{1,k}\rangle). \tag{6}$$

If the Slater rank of a quantum state is unity it is a nonentangled state, i.e., the only correlations that exist between the fermions can be attributed to their indistinguishable nature. In order to determine the Slater rank the partial trace over one of the particles is performed on the density matrix, which defines the reduced density matrix,

$$\rho_{\text{red}} = \text{Tr}_2[|\Psi\rangle\langle\Psi|] = \sum_j \langle\psi_{2,j}|\Psi\rangle\langle\Psi|\psi_{2,j}\rangle. \tag{7}$$

The Slater rank equals the rank of the reduced density matrix. For pure states of two identical fermions we consider two entanglement witnesses, the reduced von-Neumann entropy $\mathcal{E}_{\text{VN}}$ and the reduced linear entropy $\mathcal{E}_{\text{L}}$,

$$\mathcal{E}_{\text{VN}} = S[\rho_{\text{red}}] - \log_2 2, \tag{8}$$

$$\mathcal{E}_{\text{L}} = 1 - 2\,\text{Tr}\big[\rho_{\text{red}}^2\big], \tag{9}$$

where $S[\rho_{\text{red}}] = -\text{Tr}[\rho_{\text{red}}\log_2(\rho_{\text{red}})]$ is the ordinary von-Neumann entropy. Canceling the amount of entropy corresponding to the antisymmetrization of the fermionic states ($\log_2 2$ and 1, respectively) both measures vanish if and only if a state is nonentangled in the fermionic sense [22]. The advantage of (9) is that the reduced density matrix needs not be diagonalized for evaluation, therefore it is most commonly used in numerical treatments.

Up to now we have considered a general state $|\Psi\rangle$, describing two fermions, that can be written as a Slater determinant. Turning on an interaction between the fermions introduces entanglement. We will only consider interactions that do not explicitly couple the spatial and the spin degrees of freedom. Thus entanglement stems from the separability inherited by this kind of interaction, and remains, even in the noninteracting limit, as an *offset entanglement*. The spins couple to give singlet and triplet states due to the interaction as we have implicitly assumed by the choice of the symmetry operator Π_{12}. The separability of the Hamiltonian is carried forward to a product wave function and further to a product of reduced density matrices,

$$\rho_{\text{red}} = \rho_{\text{red}}^{\text{spatial}}\,\rho_{\text{red}}^{\text{spin}}. \tag{10}$$

Notice that this holds only because the one-particle basis, used to trace over the density matrix, can equivalently be expressed as product states $|\psi_{2,j}\rangle = |\psi_j(\boldsymbol{r}_2)\rangle \otimes |(S, S_z)_{2,j}\rangle$ of a spatial and a spin state. Plugging (10) into (8) and (9) we find

$$\mathcal{E}_{\text{VN}} = S\big[\rho_{\text{red}}^{\text{spatial}}\big] + S\big[\rho_{\text{red}}^{\text{spin}}\big] - 1, \tag{11}$$

$$\mathcal{E}_{\text{L}} = 1 - 2\,\text{Tr}\big[\big(\rho_{\text{red}}^{\text{spatial}}\big)^2\big]\,\text{Tr}\big[\big(\rho_{\text{red}}^{\text{spin}}\big)^2\big]. \tag{12}$$

TABLE I. The spatial entanglement between the two electrons for the lowest energy states in the COM and relative basis for the noninteracting harmonic model. We show two entanglement witnesses, the reduced von-Neumann entropy $\mathcal{E}_{\mathrm{VN}}^{\mathrm{spatial}}$ and the reduced linear entropy $\mathcal{E}_{\mathrm{L}}^{\mathrm{spatial}}$, which are zero for nonentangled states, and greater than zero for entangled states. A fermionic state is not entangled if it is the result of antisymmetrizing two orthogonal one-particle states, where we purposely consider solely the spatial wave function. Notice that the entropies of the states including spin can be obtained from the results presented by applying Eqs. (11) and (12), respectively.

E (m.u.)	m	State	$\mathcal{E}_{\mathrm{VN}}^{\mathrm{spatial}}$	$\mathcal{E}_{\mathrm{L}}^{\mathrm{spatial}}$
2	0	$\lvert 0,0,0,0\rangle^{+1}$	0.0	0.0
3	1	$\lvert 0,1,0,0\rangle^{\pm 1}$	0.0	0.0
3	1	$\lvert 0,0,0,1\rangle^{\pm 1}$	0.0	0.0
4	0	$\lvert 1,0,0,0\rangle^{+1}$	1.0	0.5
4	0	$\lvert 0,0,1,0\rangle^{+1}$	1.0	0.5
4	0	$\lvert 0,1,0,-1\rangle^{\pm 1}$	0.0	0.0
4	2	$\lvert 0,0,0,2\rangle^{\pm 1}$	1.0	0.5
4	2	$\lvert 0,2,0,0\rangle^{\pm 1}$	1.0	0.5
4	2	$\lvert 0,1,0,1\rangle^{\pm 1}$	0.0	0.0
5	1	$\lvert 0,1,0,-2\rangle^{\pm 1}$	1.29879	0.53125
5	1	$\lvert 0,1,1,0\rangle^{\pm 1}$	1.5	0.625
5	1	$\lvert 1,1,0,0\rangle^{\pm 1}$	1.29879	0.53125
5	1	$\lvert 0,0,1,1\rangle^{\pm 1}$	1.29879	0.53125
5	1	$\lvert 1,0,0,1\rangle^{\pm 1}$	1.5	0.625
5	1	$\lvert 0,2,0,-1\rangle^{\pm 1}$	1.29879	0.53125
5	3	$\lvert 0,1,0,2\rangle^{\pm 1}$	1.06128	0.40625
5	3	$\lvert 0,3,0,0\rangle^{\pm 1}$	1.56128	0.65625
5	3	$\lvert 0,0,0,3\rangle^{\pm 1}$	1.56128	0.65625
5	3	$\lvert 0,2,0,1\rangle^{\pm 1}$	1.06128	0.40625

The spin-dependent part is easily evaluated for the spin states $|S,S_z\rangle$:

$$S\left[\rho_{\mathrm{red}}^{\mathrm{spin}}(|0,0\rangle)\right] = S\left[\rho_{\mathrm{red}}^{\mathrm{spin}}(|1,0\rangle)\right] = 1,$$
$$S\left[\rho_{\mathrm{red}}^{\mathrm{spin}}(|1,+1\rangle)\right] = S\left[\rho_{\mathrm{red}}^{\mathrm{spin}}(|1,-1\rangle)\right] = 0,$$
$$\mathrm{Tr}\left[\left(\rho_{\mathrm{red}}^{\mathrm{spin}}(|0,0\rangle)\right)^2\right] = \mathrm{Tr}\left[\left(\rho_{\mathrm{red}}^{\mathrm{spin}}(|1,0\rangle)\right)^2\right] = \tfrac{1}{2},$$
$$\mathrm{Tr}\left[\left(\rho_{\mathrm{red}}^{\mathrm{spin}}(|1,+1\rangle)\right)^2\right] = \mathrm{Tr}\left[\left(\rho_{\mathrm{red}}^{\mathrm{spin}}(|1,-1\rangle)\right)^2\right] = 1,$$

and depends only on $|S_z|$. By considering the interparticle interaction with first-order perturbation theory for a fourfold degenerate subsystem the authors of [24] introduce this kind of entanglement. Independently of the confining potential these states will be entangled for $S_z = 0$. However, this effect does not explain the nonvanishing values of entanglement in atomic models with harmonic confinement for decreasing interaction strength, as they claim. Indeed another separability induces this nonvanishing entanglement.

For two distance-dependently interacting fermions in harmonic confinement the system is separable in COM and relative motion. This holds in any dimension, also for anisotropic harmonic potentials. The separability leads to the eigenstates being product states of COM and relative wave functions, which can preliminarily be incorporated. Regarding the interaction as a perturbation, the correct symmetrization of the eigenstates can be found by diagonalizing the interaction matrix in a basis of degenerate eigenstates [24].

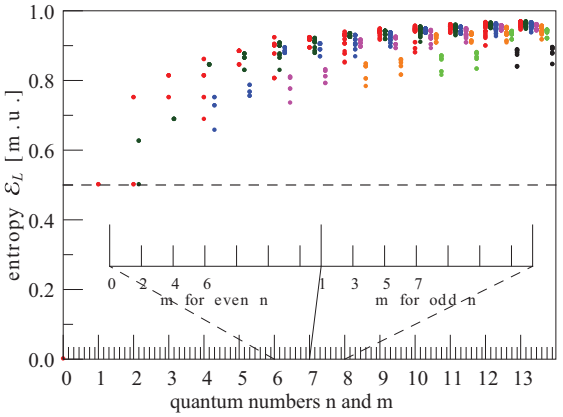

FIG. 1. (Color online) The linear entropies $\mathcal{E}_{\mathrm{L}}$ for all eigenstates in the noninteracting limit up to principal quantum number $n = 13$. Points corresponding to the same principal quantum number n, but different angular momenta m are displaced horizontally for better visibility, as indicated for $n = 6$ and 7 by the enlarged scale. The spin quantum number is set to $S_z \equiv 0$ for all states. For nonvanishing angular momentum we consider states without parity symmetrization. The dashed horizontal line corresponds to the saturation limit for the linear entropy in helium. The eigenenergies are given by $E_n = (n+2)$ m.u..

Entanglement is introduced by the symmetrization already before the interaction actually couples the two particles. As a consequence the entanglement for such systems will not generally vanish in the noninteracting limit. The explicit kind of interelectron interaction does not play a major role, as long as it depends solely on the interparticle distance. With this we include the Crandall atom and the Hooke atom discussed in [23], as well as the Moshinsky atom and a model with contact interaction addressed in [24]. Systems without explicit separability in COM and relative coordinates usually relax in a basis of independent particles and will not show such an offset entanglement. The linear entropy of helium has been shown to saturate to the value of one-half [24,26]. In contrast, the linear entropy for states in the above-mentioned atomic models with harmonic confinement saturates to the higher value of unity [24]. The linear entropy is either equal to the spatial linear entropy presented in Table I or calculated by $\mathcal{E}_L = \frac{1}{2} + \frac{1}{2}\mathcal{E}_L^{\mathrm{spatial}}$. The spatial linear entropy is calculated by considering only the spatial wave function, $\mathcal{E}_L^{\mathrm{spatial}} = 1 - 2\,\mathrm{Tr}[(\rho_{\mathrm{red}}^{\mathrm{spatial}})^2]$. For most of the states the entropies in the noninteracting case already exceed the limit for helium; see Fig. 1. The offset entanglement is thus responsible for the higher limit for the linear entropy in the harmonic cases. Furthermore the linear entropy for the interacting model has been shown to increase with the energy [24]. This dependence is already contained in the noninteracting limit (Fig. 1).

Another effect can be interpreted in terms of the offset entanglement that emerges from some separability of the considered system. For an anisotropic harmonic system with $\omega_z \gg \omega_0 = \omega_x = \omega_y$ and Coulomb interparticle interaction a magnetic field is applied [31]. As shown in [32] the primarily cylindrically symmetric system becomes spherically

symmetric for magnetic fields, such that $\omega_z \equiv \sqrt{\omega_B^2 + \omega_0^2}$, with the Larmor frequency ω_B. At this specific value a minimum of the entanglement is found for several different strengths of the confinement parameter ω_0. The states in the noninteracting limit belong either to a symmetry class of the cylindrical or of the spherical symmetry. Qualitatively speaking the interaction does affect the states differently according to their algebraic properties. We expect that the offset entanglement is different, depending on the symmetry. In particular, we expect the spherically symmetric representation to be less entangled than the cylindrically symmetric one. This discontinuity in the noninteracting limit carries forward to a minimum in the interacting case.

IV. HARMONIC CONFINING POTENTIAL

We discuss the harmonic case (V_{harmonic}) for two reasons. First we show that HFR is not applicable for the planar model, except for one particular case, which includes both parities. Then we use this case as an illustrative example and to introduce basic concepts that will clarify the origin of the *alternating rule* in the quartic case.

The harmonic two-electron quantum dot model is separable in COM and relative motion and the associated potentials are radially symmetric. Therefore, the angular momenta in these two separate dynamics are good quantum numbers. We construct a basis with two pairs of quantum numbers (n_c, m_c) and (n_r, m_r) associated with the polar COM and relative coordinates, respectively:

$$|n_c,m_c,n_r,m_r\rangle^{\epsilon_p} = \frac{1}{\sqrt{2}}(|n_c,m_c,n_r,m_r\rangle + \epsilon_p|n_c,-m_c,n_r,-m_r\rangle).$$

The eigenvalues of the symmetry operators in this basis are $m = |m_c + m_r|$, $\epsilon_s = (-1)^{m_r}$, and $\epsilon_p = \pm 1$.

Understanding the applicability of HFR for the harmonic case requires the identification of states that arise from the same configuration of one-electron orbitals. This, however, is not a trivial task due to the separability in the chosen coordinates. The fermionic entanglement for indistinguishable particles [30] can be used for this purpose. At this point it is necessary to clearly distinguish our application from the general term of entanglement, as presented in the last section. Our goal is to identify states that are the direct antisymmetrization of one-particle orbitals, as stated in the empiric definition of HFR [3]. This rule is valid in the nonrelativistic limit, where no coupling between spatial and spin degrees of freedom is presumed. Consequently, we do not consider the spin-dependent part of the wave function at all, as it has no influence on the energy of the state. The ambiguities here are easily explained with an example. The state $|0,1,0,0\rangle^{+1}$ can be expressed with a Slater decomposition of rank unity and gives $\mathcal{E}_{\text{VN}} = 0$ in the noninteracting limit. Taking into consideration also the spin-dependent wave function, which is singlet, the state is indeed entangled in the fermionic sense, since

$$\mathcal{E}_{\text{VN}}[|0,1,0,0\rangle^{+1} \otimes |0,0\rangle] = 1. \quad (13)$$

The corresponding state of helium is the $(1s2p)\,^1P$ state, for which HFR is applicable in combination with the triplet state $(1s2p)\,^3P$. A unique case is the ground state, for which we find $\mathcal{E}_{\text{VN}}[|0,0,0,0\rangle^{+1}] = -1$, since the antisymmetrization is exclusively contained in the spin wave function. This will be of no further concern to us, since there cannot be a corresponding triplet state for the ground state.

In the last section we explained, that already the choice of the appropriate symmetry class creates entanglement of the states. The symmetry and the exact quantum numbers n_c, m_c, n_r, m_r are independent of the value of γ. We have thus found a possible choice of symmetry class induced by the interaction. For nonvanishing angular momenta, omitting the parity and allowing negative values for m offers another choice of an appropriate basis. For $\gamma = 0$ the entanglement between the two fermionic particles in terms of the quantum numbers describing the state $|n_c,m_c,n_r,m_r\rangle^{\epsilon_p}$ can be calculated analytically (see Appendix B). We consider the density matrix,

$$|\psi\rangle\langle\psi| = |n_c,m_c,n_r,m_r\rangle^{\epsilon_p\ \epsilon_p}\langle n_c,m_c,n_r,m_r|, \quad (14)$$

and represent it in an independent-particle basis. The trace over one particle leads to the reduced density matrix ρ_{red}. In Table I we show the reduced spatial von-Neumann entropy $\mathcal{E}_{\text{VN}}^{\text{spatial}}$ and the reduced spatial linear entropy $\mathcal{E}_{\text{L}}^{\text{spatial}}$ for various eigenstates. We have tested all states up to $E = 15$ m.u. for the noninteracting case, and the only pairs of spatially nonentangled singlet and triplet states we found are $|0,1,0,0\rangle^{\epsilon_p}$ and $|0,0,0,1\rangle^{\epsilon_p}$. Here the even- and odd-parity states are degenerate, so we only consider the even case $\epsilon_p = 1$. Notice that we have also tested the entanglement for the more common second choice of positive and negative angular momenta. The only spatially nonentangled pairs we found are the corresponding pairs ($|1,0,0,0\rangle$,$|0,0,1,0\rangle$) with $m = 1$ and ($|0,1,0,0\rangle$,$|0,0,0,1\rangle$) with $m = -1$.

These states follow HFR and the singlet energy grows larger than the corresponding triplet energy with adiabatically increasing the interparticle interaction. We show the details of this effect by considering the different parts, which contribute to the total energy in Fig. 2. We observe that the total energy, the Coulomb energy, and the confining harmonic energy are higher for the singlet state. In contrast to the atomic case, Slater's explanation generally holds for the harmonic quantum dot:

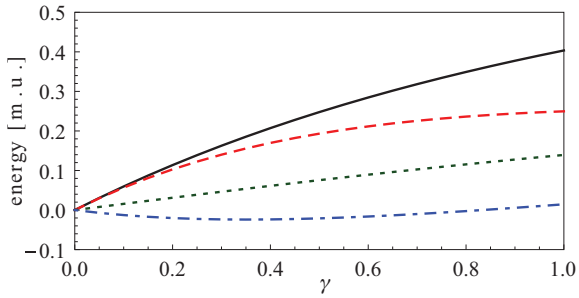

FIG. 2. (Color online) Energy difference between the singlet state $|0,1,0,0\rangle^{+1}$ and the triplet state $|0,0,0,1\rangle^{+1}$ for the harmonic confining potential. Adiabatically raising the interparticle interaction via the Coulomb strength parameter γ lifts the degeneracy of the singlet and triplet states for total energy (solid line), Coulomb potential (dashed line), harmonic potential (dotted line), and kinetic energy (dot-dashed line).

The Fermi hole causes the lower value of the triplet Coulomb interaction.

In order to understand the origin of the Fermi hole we take a deeper look at the structure of the effective potential. This potential consists of the ordinary potential and the dynamic part coming from the angular solution which corresponds to the classical angular momentum barrier. The antisymmetry under interparticle exchange imposes even (odd) values of the angular momentum quantum number in relative coordinates m_r for the singlet (triplet) case. The effective potential depends on these quantum numbers and thus on the symmetrization and, already for the noninteracting case, determines the localization properties of the state. This localization is responsible for the amount of influence of the Coulomb interaction. In the example considered, the singlet state has vanishing angular momentum in the relative coordinate, while for the triplet state $m_r = \pm 1$. In general it may well be possible, that a singlet state has higher relative angular momentum than the corresponding triplet state which would cause a violation of Hund's rule.

The localization of these states, their corresponding effective potentials, and influences of the Coulomb potential are illustrated in Fig. 3. The singlet state localizes close to the origin in the relative coordinate, because it does not feel an angular momentum barrier in this coordinate (top, left panel). The Coulomb term thus has a large influence on the singlet state and the expectation value of the Coulomb interaction reads

$$^{+1}\langle 0,1,0,0|\frac{1}{r_{\rm rel}}|0,1,0,0\rangle^{+1} = \sqrt{\frac{\pi}{2}}\,\text{m.u.} \qquad (15)$$

In addition, the Coulomb barrier changes the effective potential and the localization of the state as shown in Fig. 3 (top, right panel). The triplet state has no probability of presence close to the origin of the relative coordinate (bottom, left panel), which is reflected in a smaller value of the Coulomb interaction compared with the singlet case,

$$^{+1}\langle 0,0,0,1|\frac{1}{r_{\rm rel}}|0,0,0,1\rangle^{+1} = \sqrt{\frac{\pi}{8}}\,\text{m.u.} \qquad (16)$$

In the interacting case only minor changes in the effective potential and the localization can be observed in Fig. 3 (bottom, right panel).

The rather low dependence of the localization of both states on the Coulomb interaction suggests application of first-order perturbation theory. The energy levels depend nearly linearly on γ; see Fig. 4(a), particularly for the triplet state, and the deviation is quadratic in γ [see Fig. 4(b)], and is well described with second-order perturbation theory for both cases.

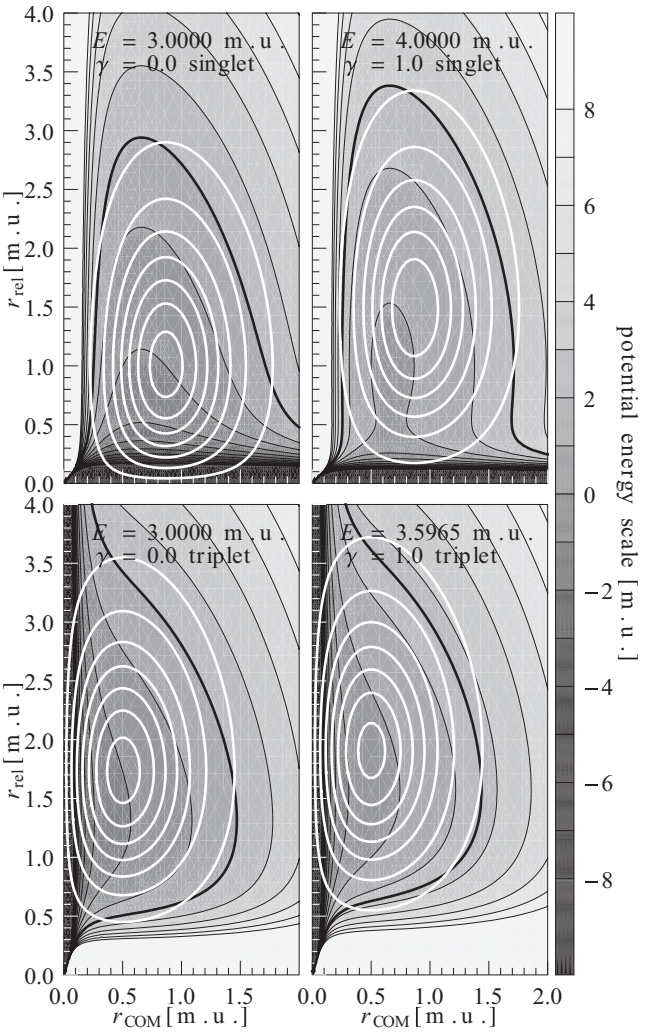

FIG. 3. The probability density of the singlet state $|0,1,0,0\rangle^{+1}$ (top) and the triplet state $|0,0,0,1\rangle^{+1}$ (bottom) in the noninteracting ($\gamma = 0$, left) and interacting ($\gamma = 1$, right) harmonic case is pictured here. The angular dependencies have been integrated out [27]. The gray shadings represent the confining effective potential with the thick equipotential line equal to the eigenenergy of the state. The white lines are contour lines of the probability density starting from 0.05 in steps of 0.1. The probability density of the singlet state is localized close to the origin of the relative coordinates for the non-interacting case (top, left) and therefore significantly affected by the Coulomb interaction (top, right). The triplet state is localized close to the origin of the COM coordinate, but the angular momentum barrier in the relative coordinate repels the wave function from the origin (bottom, left). The Coulomb interaction causes only minor changes in the effective potential and in the localization of the triplet state (bottom, right).

V. QUARTIC CONFINING POTENTIAL

For the quartic confining potential $V_{\rm quartic}$ the separability in COM and relative motion is lost. Still we can express the potential in the coordinates $r_{\rm COM}$, $r_{\rm rel}$, and $\varphi = \varphi_{\rm COM} - \varphi_{\rm rel}$, such that the confining potential is given by

$$V_{\rm quartic}(r_{\rm COM}, r_{\rm rel}, \varphi) = 2\, r_{\rm COM}^4 + \tfrac{1}{8}\, r_{\rm rel}^4 + r_{\rm COM}^2 r_{\rm rel}^2 (3 - 2\sin^2\varphi). \qquad (17)$$

There is no dependence on the angle $\vartheta = \varphi_{\rm COM} + \varphi_{\rm rel}$, which is the conjugate coordinate to the conserved total angular momentum perpendicular to the plane.

For potentials lacking a further separation, apart from the separation in independent particles for the noninteracting case, there is no subtlety about the applicability of HFR. This is also valid for the quartic potential. All states arise from (anti-)symmetrization of one-particle orbitals and the noninteracting eigenenergies can be expressed as the sum of

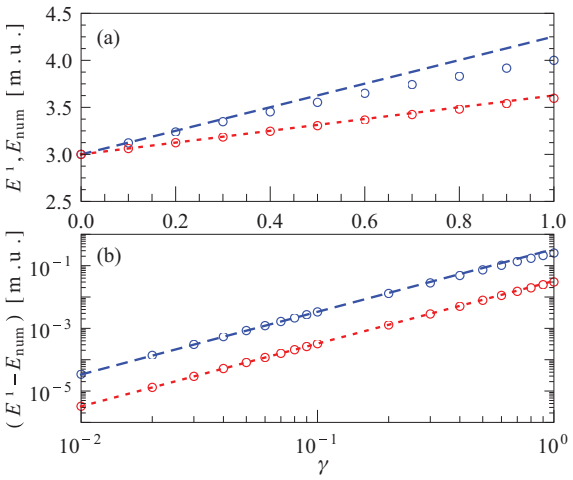

FIG. 4. (Color online) For the harmonic confinement the numerically exact eigenenergies $E_{\rm num}$ (circles) and the results from first-order perturbation theory E^1 (lines) are shown in (a). The singlet state has higher energy than the triplet state. Both can be approximated by first-order perturbation theory (singlet: dashed line; triplet: dotted line). The deviation $E^1 - E_{\rm num}$ is shown in (b). The numerical values (circles) are close to the quadratic fit for the triplet (dotted) and the singlet case (dashed). Small deviations are observed close to $\gamma = 1$. The magnitude of the quadratic deviation of the singlet state is larger by a factor of approximately ten, in accordance with the significant change in the wave function (compare Fig. 3).

the one-particle solutions. For the planar quartic confinement the one-particle problem is radially symmetric and solutions are provided by Ref. [33] with principal quantum number n_j and angular momentum quantum number m_j, where j denotes the particle. We construct the two-electron basis by

$$|n_1,m_1,n_2,m_2\rangle_{\rm ind}^{\epsilon_p,\epsilon_s} = \tfrac{1}{2}[(|n_1,m_1,n_2,m_2\rangle_{\rm ind} + \epsilon_p|n_1,-m_1,n_2,-m_2\rangle_{\rm ind}) + \epsilon_s(|n_2,m_2,n_1,m_1\rangle_{\rm ind} + \epsilon_p|n_2,-m_2,n_1,-m_1\rangle_{\rm ind})], \quad (18)$$

with the eigenvalues ϵ_p for the parity operator, ϵ_s for the particle exchange operator, and $(m_1+m_2)^2$ for L_z^2. In order to distinguish the basis in COM and relative coordinates from the independent particle basis we introduce the subscript "ind" for the latter.

For two independent particles with vanishing total angular momentum we find three different classes of states for which

TABLE II. Numerical results for the states $|1,1,0,-1\rangle_{\rm ind}^{\epsilon_p,\epsilon_s}$ for the quartic potential. All four states are degenerate for the noninteracting case with the energy $E = 12.098604$ m.u.. The approximate quantum numbers are used to calculate the effective potential in Figs. 6 and 7. The expectation value of the Coulomb potential is used for the calculation of first-order perturbation theory in Fig. 8.

Spin	Parity	$\tilde{m}_{\rm rel}$	$\langle 1/r_{\rm rel}\rangle$ (m.u.)	$E(\gamma = 1)$ (m.u.)
Singlet	Even	0.2269	1.711000091	13.65192024
Triplet	Even	1.0090	0.966742637	13.03986337
Singlet	Odd	2.0136	0.761620656	12.85001951
Triplet	Odd	1.0745	0.947045869	13.02380571

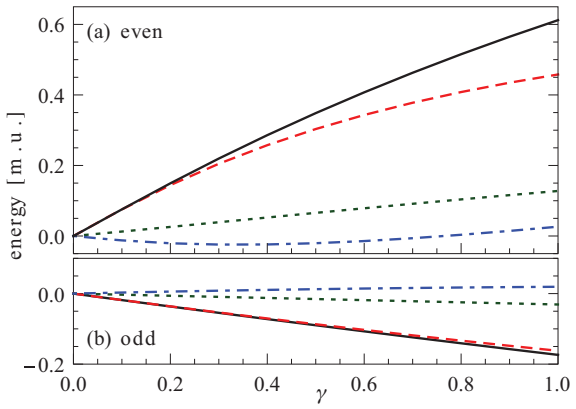

FIG. 5. (Color online) Energy differences between singlet and triplet states for total energy (solid line), Coulomb potential (dashed line), quartic potential (dotted line), and kinetic energy (dot-dashed line). (a) Shows states with even parity $|1,1,0,-1\rangle_{\rm ind}^{+1,\pm1}$; (b) shows states with odd parity $|1,1,0,-1\rangle_{\rm ind}^{-1,\pm1}$. The lowest states with zero angular momentum follow the *alternating rule*; the even singlet state has higher energy than the even triplet state while the odd singlet state has lower energy than the odd triplet state. The Coulomb potential follows the same trend as the total energy.

HFR can be applied. There are pairs of singlet and triplet states with even parity and pairs with odd parity. Furthermore, there are states of the form $|n_1,m_1,n_1,-m_1\rangle_{\rm ind}^{\pm1,\pm1}$ which give rise to pairs of mixed parity, namely singlet even-parity states corresponding to triplet odd-parity states. In the quartic

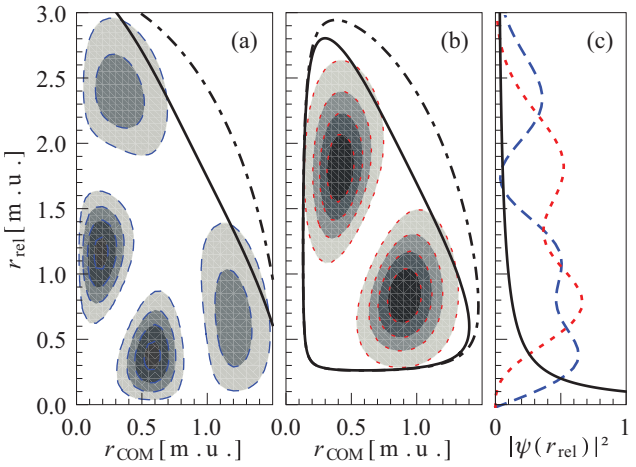

FIG. 6. (Color online) The probability density of the singlet (a) and triplet state (b) $|1,1,0,-1\rangle_{\rm ind}^{+1,\pm1}$ with even parity in COM and relative radial distance for the noninteracting case ($\gamma = 0$) confined by a quartic potential. The angles are integrated out. The thick lines are the equipotential lines equal to the eigenenergy of the effective potential (solid line, $\sin^2\varphi = 0$; dot-dashed line, $\sin^2\varphi = 1$) with the numerically obtained approximate angular quantum numbers $\tilde{m}_c$ and $\tilde{m}_r$. The projection (integration over $r_{\rm COM}$) on the relative distance (c) shows the different effect of the Coulomb potential (schematic, solid line) on the singlet (dashed line) and the triplet (dotted line) state. The Coulomb potential has a larger effect on the singlet than on the triplet state, as a consequence of the different approximate relative quantum numbers of $\tilde{m}_r \approx 0$ and $\tilde{m}_r \approx 1$, respectively.

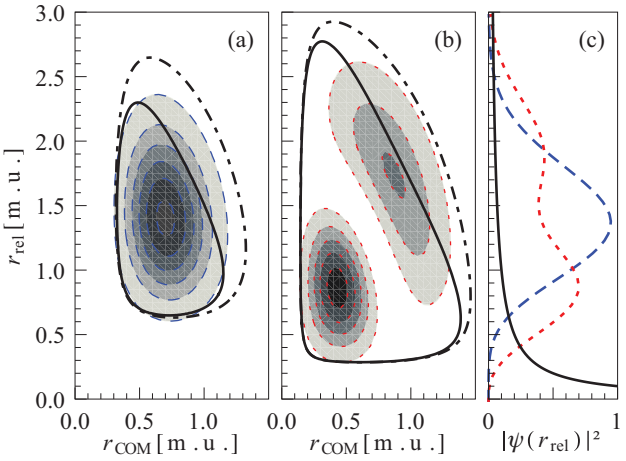

FIG. 7. (Color online) The probability density of the singlet (a) and triplet state (b) $|1,1,0,-1\rangle_{\mathrm{ind}}^{-1,\pm1}$ with odd parity; settings equal those in Fig. 6. Again the projection on the relative distance (c) shows the different effect of the Coulomb potential. The *alternating rule* can be explained with the approximate quantum number $\tilde{m}_r \approx 2$ for the odd singlet state, while the odd triplet state has $\tilde{m}_r \approx 1$.

confining potential we consider 110 states in total, where the highest level is the state $|3,0,3,0\rangle_{\mathrm{ind}}^{+1,+1}$ with eigenenergy $E = 36.917640$ m.u.. Within this range there are 25 even-parity pairs and 12 mixed-parity pairs. For all of those the singlet energy is higher than the corresponding triplet energy. For the 16 odd-parity states considered the behavior is inverted and all triplet energies are higher than the corresponding singlet energies. Therefore HFR holds for all the even and mixed-parity pairs, while the odd-parity pairs violate the rule. A similar effect can be observed for helium, which was investigated in [3] and led to the formulation of the *alternating rule*. This rule states that for unnatural parity states, corresponding to odd states for vanishing angular momentum, HFR is reversed, such that singlet states are lower in energy than the associated triplet states.

To understand this behavior we follow the line of argumentation from the harmonic case. As an example we pick the first pair of states that shows the violation $|n_1,m_1,n_2,m_2\rangle_{\mathrm{ind}}^{\epsilon_p,\epsilon_s} = |1,1,0,-1\rangle_{\mathrm{ind}}^{-1,\pm1}$. We compare these states with the degenerate pair of even states $|n_1,m_1,n_2,m_2\rangle_{\mathrm{ind}}^{\epsilon_p,\epsilon_s} = |1,1,0,-1\rangle_{\mathrm{ind}}^{+1,\pm1}$. The common eigenenergy for the noninteracting case is

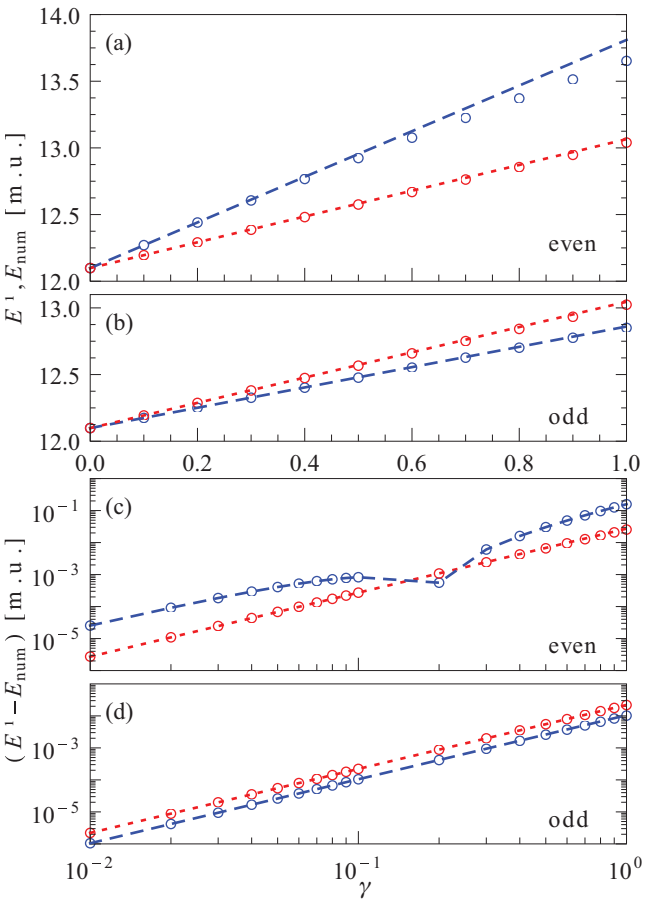

FIG. 8. (Color online) For quartic confinement the numerically exact eigenenergies E_{num} (circles) and results from first-order perturbation theory E^1 (lines) are shown in (a) and (b) for even and odd states, respectively. The deviation $E^1 - E_{\mathrm{num}}$ is shown in (c) and (d), for even and odd states, respectively. For the singlet even case, the dashed line is a guide to the eye, while for the other cases the lines are the quadratic fit. For these cases the behavior of the states confined by a quartic potential can be understood considering first-order perturbation theory. The singlet even state, like in the harmonic potential, is significantly changed by the interaction potential.

$E = 12.098604$ m.u., while the energies for the interacting case are given in Table II. Again we start with considering the

TABLE III. For the quartic confinement all states considered with vanishing angular momentum follow the *alternating rule*. We show six examples of states, which are degenerate for the noninteracting case and split into four states, one in each symmetry class, when turning on the interaction. The behavior of the energies is closely related to the approximate angular momentum quantum number in relative coordinates $\tilde{m}_{\mathrm{rel}}$.

$\epsilon_p,\epsilon_s \rightarrow$	$\pm1,\pm1$	$+1,+1$	$+1,-1$	$-1,-1$	$-1,+1$	$+1,+1$	$+1,-1$	$-1,-1$	$-1,+1$
States $\downarrow$	$E\ (\gamma=0)$ (m.u.)	$\tilde{m}_{\mathrm{rel}}\ (\gamma=0)$				$E\ (\gamma=1)$ (m.u.)			
$\lvert 1,1,0,-1\rangle_{\mathrm{ind}}^{\epsilon_p,\epsilon_s}$	12.098 604	0.227	1.009	1.074	2.014	13.651 920	13.039 863	13.023 806	12.850 020
$\lvert 1,2,0,-2\rangle_{\mathrm{ind}}^{\epsilon_p,\epsilon_s}$	17.159 089	1.062	2.015	1.062	2.015	18.380 186	17.964 433	18.070 037	17.909 929
$\lvert 2,1,0,-1\rangle_{\mathrm{ind}}^{\epsilon_p,\epsilon_s}$	18.375 959	1.047	1.069	2.071	2.104	19.820 331	19.352 300	19.212 249	19.140 113
$\lvert 1,3,0,-3\rangle_{\mathrm{ind}}^{\epsilon_p,\epsilon_s}$	22.599 343	1.284	2.364	1.284	2.364	23.734 568	23.359 149	23.487 848	23.325 314
$\lvert 2,1,1,-1\rangle_{\mathrm{ind}}^{\epsilon_p,\epsilon_s}$	23.678 262	1.028	1.982	2.042	3.576	24.938 356	24.515 878	24.524 989	24.331 156
$\lvert 2,2,0,-2\rangle_{\mathrm{ind}}^{\epsilon_p,\epsilon_s}$	23.869 758	2.061	2.088	2.061	2.088	25.105 915	24.699 766	24.717 959	24.634 682

TABLE IV. For the full potential (20) we show all states with vanishing angular momentum up to the fourth state that exists only as singlet even $|3,0,3,0\rangle_{\rm ind}^{+1,+1}$. All pairs of singlet and triplet spin symmetry presented here follow the *alternating rule*. For the parity mixing pairs the singlet has higher eigenenergy than the triplet in all cases.

$\epsilon_p,\epsilon_s \rightarrow$	$\pm1,\pm1$	$+1,+1$	$+1,-1$	$-1,-1$	$-1,+1$
States $\downarrow$	$E\ (\gamma=0)$ (m.u.)		$E\ (\gamma=1)$ (m.u.)		
$\|0,0,0,0\rangle_{\rm ind}^{\epsilon_p,\epsilon_s}$	2.300376	3.445300			
$\|0,1,0,-1\rangle_{\rm ind}^{\epsilon_p,\epsilon_s}$	4.828681	5.901348		5.526039	
$\|1,0,0,0\rangle_{\rm ind}^{\epsilon_p,\epsilon_s}$	5.026830	6.210941	5.745411		
$\|0,2,0,-2\rangle_{\rm ind}^{\epsilon_p,\epsilon_s}$	7.544645	8.304078		8.221913	
$\|1,0,1,0\rangle_{\rm ind}^{\epsilon_p,\epsilon_s}$	7.753283	8.658231			
$\|1,1,0,-1\rangle_{\rm ind}^{\epsilon_p,\epsilon_s}$	7.809767	8.939785	8.507135	8.509367	8.374 386
$\|2,0,0,0\rangle_{\rm ind}^{\epsilon_p,\epsilon_s}$	8.205149	9.297429	8.932604		
$\|0,3,0,-3\rangle_{\rm ind}^{\epsilon_p,\epsilon_s}$	10.422142	11.168524		11.067339	
$\|1,2,0,-2\rangle_{\rm ind}^{\epsilon_p,\epsilon_s}$	10.743092	11.550716	11.311839	11.346638	11.298 899
$\|1,1,1,-1\rangle_{\rm ind}^{\epsilon_p,\epsilon_s}$	10.790854	11.660480		11.437097	
$\|2,0,1,0\rangle_{\rm ind}^{\epsilon_p,\epsilon_s}$	10.931602	11.915729	11.544597		
$\|2,1,0,-1\rangle_{\rm ind}^{\epsilon_p,\epsilon_s}$	11.169260	12.255326	11.884325	11.804700	11.736 365
$\|3,0,0,0\rangle_{\rm ind}^{\epsilon_p,\epsilon_s}$	11.718736	12.694313	12.429348		
$\|0,4,0,-4\rangle_{\rm ind}^{\epsilon_p,\epsilon_s}$	13.442625	14.161967		14.063219	
$\|1,3,0,-3\rangle_{\rm ind}^{\epsilon_p,\epsilon_s}$	13.811615	14.545183	14.356594	14.452876	14.341 369
$\|1,2,1,-2\rangle_{\rm ind}^{\epsilon_p,\epsilon_s}$	13.941538	14.605366		14.518543	
$\|2,0,2,0\rangle_{\rm ind}^{\epsilon_p,\epsilon_s}$	14.109921	14.864683			
$\|2,1,1,-1\rangle_{\rm ind}^{\epsilon_p,\epsilon_s}$	14.150347	15.029219	14.762885	14.756618	14.625 066
$\|2,2,0,-2\rangle_{\rm ind}^{\epsilon_p,\epsilon_s}$	14.268852	15.116291	14.849053	14.906673	14.830 529
$\|3,0,1,0\rangle_{\rm ind}^{\epsilon_p,\epsilon_s}$	14.445189	15.433439	15.088643		
$\|3,1,0,-1\rangle_{\rm ind}^{\epsilon_p,\epsilon_s}$	14.828671	15.814453	15.532502	15.412681	15.379 656
$\|4,0,0,0\rangle_{\rm ind}^{\epsilon_p,\epsilon_s}$	15.507363	16.388931	16.196457		
$\|0,5,0,-5\rangle_{\rm ind}^{\epsilon_p,\epsilon_s}$	16.592132	17.286283		17.192212	
$\|1,4,0,-4\rangle_{\rm ind}^{\epsilon_p,\epsilon_s}$	17.003417	17.738025	17.524732	17.626659	17.512 953
$\|1,3,1,-3\rangle_{\rm ind}^{\epsilon_p,\epsilon_s}$	17.201089	17.825499		17.750490	
$\|2,2,1,-2\rangle_{\rm ind}^{\epsilon_p,\epsilon_s}$	17.467298	18.143407	17.959234	17.993150	17.948 675
$\|2,3,0,-3\rangle_{\rm ind}^{\epsilon_p,\epsilon_s}$	17.490745	18.232610	18.045281	18.060870	18.028 437
$\|2,1,2,-1\rangle_{\rm ind}^{\epsilon_p,\epsilon_s}$	17.509840	18.262858		18.125871	
$\|3,0,2,0\rangle_{\rm ind}^{\epsilon_p,\epsilon_s}$	17.623508	18.476730	18.175475		
$\|3,1,1,-1\rangle_{\rm ind}^{\epsilon_p,\epsilon_s}$	17.809757	18.752802	18.458853	18.386646	18.304 178
$\|3,2,0,-2\rangle_{\rm ind}^{\epsilon_p,\epsilon_s}$	18.065858	18.820033	18.635417	18.650041	18.613 835
$\|4,0,1,0\rangle_{\rm ind}^{\epsilon_p,\epsilon_s}$	18.233816	19.157663	18.875963		
$\|4,1,0,-1\rangle_{\rm ind}^{\epsilon_p,\epsilon_s}$	18.741379	19.630870	19.426534	19.291770	19.274 082
$\|5,0,0,0\rangle_{\rm ind}^{\epsilon_p,\epsilon_s}$	19.532674	20.344307	20.200976		
$\|0,6,0,-6\rangle_{\rm ind}^{\epsilon_p,\epsilon_s}$	19.859704	20.531683		20.442313	
$\|1,5,0,-5\rangle_{\rm ind}^{\epsilon_p,\epsilon_s}$	20.308870	21.017504	20.810666	20.912889	20.801 416
$\|1,4,1,-4\rangle_{\rm ind}^{\epsilon_p,\epsilon_s}$	20.564210	21.164293		21.094610	
$\|3,3,0,-3\rangle_{\rm ind}^{\epsilon_p,\epsilon_s}$	20.824908	21.499174	21.341913	21.393522	21.329 198
$\|2,3,1,-3\rangle_{\rm ind}^{\epsilon_p,\epsilon_s}$	20.880218	21.523390	21.375837	21.464398	21.358 846
$\|2,2,2,-2\rangle_{\rm ind}^{\epsilon_p,\epsilon_s}$	20.993059	21.602197		21.517722	
$\|3,0,3,0\rangle_{\rm ind}^{\epsilon_p,\epsilon_s}$	21.137096	21.796490			

virial theorem, Eq. (5), and the splitting of the eigenenergy in kinetic, quartic, and Coulomb potential energies (see Fig. 5). In both cases the potential energies support the trend of the total energy. This is expected for the even-parity case, but surprising for the odd case. Although one pair follows the rule, while the other violates it, the effect appears to have the same origin.

The investigation in the COM and relative coordinates offered an insight for the harmonic potential, so it appears to be reasonable to consider the same for the quartic potential. We neglect the term depending on the angle φ in Eq. (17) for a moment and assume the solution,

$$\frac{1}{2\pi}\exp[i(\tilde{m}_{\rm COM}\varphi_{\rm COM}+\tilde{m}_{\rm rel}\varphi_{\rm rel})],$$

for the angular part in the COM and the relative motion with the approximate not necessarily integer valued quantum numbers $\tilde{m}_{\rm COM}$ and $\tilde{m}_{\rm rel}$. We determine numerically the values of these approximate quantum numbers by evaluating the expressions $|\tilde{m}_{\rm COM}|=\sqrt{\langle\psi|\partial^2_{\varphi_{\rm COM}}|\psi\rangle}$ and $|\tilde{m}_{\rm rel}|=\sqrt{\langle\psi|\partial^2_{\varphi_{\rm rel}}|\psi\rangle}$. The results preserve the total angular momentum to the extent that $m=||\tilde{m}_{\rm COM}|\pm|\tilde{m}_{\rm rel}||$. The approximate effective potential

including the dependence on the angle φ reads

$$V_{\rm eff}(r_{\rm COM}, r_{\rm rel}, \varphi) = -\frac{1/4 - \tilde{m}^2_{\rm COM}}{4r^2_{\rm COM}} - \frac{1/4 - \tilde{m}^2_{\rm rel}}{r^2_{\rm rel}} + \frac{\gamma}{r_{\rm rel}} + 2\,r^4_{\rm COM} + \frac{1}{8}\,r^4_{\rm rel} + r^2_{\rm COM} r^2_{\rm rel}(3 - 2\sin^2\varphi). \quad (19)$$

In Figs. 6 and 7 we show the limiting cases for $\sin^2\varphi = 0$ (solid line) and $\sin^2\varphi = 1$ (dot-dashed line). The numerically obtained wave functions fit very well into these approximate effective potentials. The high angular excitation for the odd singlet state explains the violation of HFR. The angular momentum barrier shapes the localization of the state such that it has only weak overlap with the Coulomb potential, which becomes obvious when considering the projection of the wave function on the relative radial coordinate alone; see Fig. 7(c).

Finally, we also consider first-order perturbation theory for the quartic confinement. The expectation values of the Coulomb potential for the noninteracting eigenstates can be calculated numerically (see Table II). The energies calculated by first-order perturbation theory are in good agreement with the numerically exact results; see Figs. 8(a) and 8(b). The deviation is quadratic in γ for most cases; see Figs. 8(c) and 8(d), except for the singlet state with even parity. Here the deviation is not quadratic, which means that the localization of the wave function is significantly changed by the interparticle interaction.

The *alternating rule* is applicable for all singlet-triplet pairs of states with vanishing angular momentum and is valid in an energy regime up to approximately $E = 32$ m.u. (see Table III). For planar confinement the even- and odd-parity states for nonvanishing angular momentum correspond to negative and positive angular momenta and are degenerate. It is not meaningful to apply the *alternating rule* for these cases. Nevertheless, HFR is generally fulfilled, with some exceptions, e.g. when certain corresponding singlet and triplet levels cross for strong correlation $\gamma > 1$; Hund's rules were never assumed to be valid for strongly correlated states. Considering the range for the Coulomb strength parameter γ for the case with GaAs (see Appendix A) this is still in the physically relevant regime.

VI. OTHER CONFINEMENTS

Finally, we consider harmonic confinement with a quartic perturbation which accounts for a realistic deviation from the well-established harmonic model [20]. With modified units corresponding to the harmonic potential the full confining potential reads

$$V_{\rm full}(\boldsymbol{r}) = \tfrac{1}{2}\boldsymbol{r}^2 + \kappa(\boldsymbol{r}^2)^2, \quad (20)$$

TABLE V. For the billiard potential $V_{\rm billiard}$ we show unperturbed energies and the first- and second-order corrections for the first 67 states in all four symmetry classes with vanishing angular momentum. Values are given in modified units. All presented states follow the *alternating rule* considering full Coulomb interaction ($\gamma = 1$).

$\epsilon_p,\epsilon_s \rightarrow$	$\pm1,\pm1$	$+1,+1$		$+1,-1$		$-1,-1$		$-1,+1$	
States $\downarrow$	$E\ (\gamma = 0)$	$O(\gamma)$	$O(\gamma^2)$	$O(\gamma)$	$O(\gamma^2)$	$O(\gamma)$	$O(\gamma^2)$	$O(\gamma)$	$O(\gamma^2)$
$\lvert 0,0,0,0\rangle^{\epsilon_p,\epsilon_s}_{\rm ind}$	5.783 186	2.596	−0.96						
$\lvert 0,1,0,-1\rangle^{\epsilon_p,\epsilon_s}_{\rm ind}$	14.681 971	3.322	−0.70			0.903	−0.08		
$\lvert 1,0,0,0\rangle^{\epsilon_p,\epsilon_s}_{\rm ind}$	18.127 224	3.120	−0.61	1.660	−0.09				
$\lvert 0,2,0,-2\rangle^{\epsilon_p,\epsilon_s}_{\rm ind}$	26.374 616	2.747	−0.26			1.207	−0.05		
$\lvert 1,0,1,0\rangle^{\epsilon_p,\epsilon_s}_{\rm ind}$	30.471 262	2.481	−0.35						
$\lvert 1,1,0,-1\rangle^{\epsilon_p,\epsilon_s}_{\rm ind}$	31.950 213	3.921	−0.49	1.908	−0.07	1.908	−0.09	1.178	-0.03
$\lvert 2,0,0,0\rangle^{\epsilon_p,\epsilon_s}_{\rm ind}$	40.335 096	2.815	−0.36	1.923	−0.08				
$\lvert 0,3,0,-3\rangle^{\epsilon_p,\epsilon_s}_{\rm ind}$	40.706 466	2.510	0.05			1.323	−0.04		
$\lvert 1,2,0,-2\rangle^{\epsilon_p,\epsilon_s}_{\rm ind}$	48.612 308	3.136	−0.27	1.636	−0.06	1.636	−0.04	1.351	-0.03
$\lvert 1,1,1,-1\rangle^{\epsilon_p,\epsilon_s}_{\rm ind}$	49.218 456	3.279	−0.40			1.134	−0.03		
$\lvert 2,0,1,0\rangle^{\epsilon_p,\epsilon_s}_{\rm ind}$	52.679 135	3.092	−0.08	1.658	0.00				
$\lvert 0,4,0,-4\rangle^{\epsilon_p,\epsilon_s}_{\rm ind}$	57.582 941	2.380	0.18			1.388	−0.02		
$\lvert 2,1,0,-1\rangle^{\epsilon_p,\epsilon_s}_{\rm ind}$	59.090 712	3.533	−0.29	2.193	−0.07	2.193	−0.09	1.250	-0.03
$\lvert 1,3,0,-3\rangle^{\epsilon_p,\epsilon_s}_{\rm ind}$	67.992 019	2.797	0.12	1.539	−0.01	1.539	−0.02	1.395	-0.02
$\lvert 1,2,1,-2\rangle^{\epsilon_p,\epsilon_s}_{\rm ind}$	70.849 999	2.743	−0.75			1.427	−0.03		
$\lvert 3,0,0,0\rangle^{\epsilon_p,\epsilon_s}_{\rm ind}$	72.411 735	2.693	0.06	2.032	−0.08				
$\lvert 2,0,2,0\rangle^{\epsilon_p,\epsilon_s}_{\rm ind}$	74.887 007	2.439	−0.28						
$\lvert 2,1,1,-1\rangle^{\epsilon_p,\epsilon_s}_{\rm ind}$	76.358 955	4.084	−0.34	2.001	−0.02	2.001	−0.03	1.238	-0.01
$\lvert 0,5,0,-5\rangle^{\epsilon_p,\epsilon_s}_{\rm ind}$	76.938 928	2.299	0.57			1.432	−0.01		
$\lvert 2,2,0,-2\rangle^{\epsilon_p,\epsilon_s}_{\rm ind}$	80.697 663	2.833	−0.06	1.823	−0.05	1.823	−0.04	1.438	-0.03
$\lvert 3,0,1,0\rangle^{\epsilon_p,\epsilon_s}_{\rm ind}$	84.755 773	2.812	0.10	1.901	0.01				
$\lvert 1,4,0,-4\rangle^{\epsilon_p,\epsilon_s}_{\rm ind}$	90.005 368	2.602	0.25	1.497	0.01	1.497	0.01	1.414	-0.01
$\lvert 1,3,1,-3\rangle^{\epsilon_p,\epsilon_s}_{\rm ind}$	95.277 573	2.509	−0.95			1.519	−0.03		
$\lvert 3,1,0,-1\rangle^{\epsilon_p,\epsilon_s}_{\rm ind}$	96.101 369	3.363	0.59	2.328	−0.07	2.328	−0.09	1.235	-0.02
$\lvert 0,6,0,-6\rangle^{\epsilon_p,\epsilon_s}_{\rm ind}$	98.726 272	2.243	0.21			1.466	0.01		
$\lvert 2,2,1,-2\rangle^{\epsilon_p,\epsilon_s}_{\rm ind}$	102.935 354	3.329	−0.62	1.743	−0.07	1.743	−0.01	1.436	-0.01

where we take $\kappa = 0.1$ in our model calculations. We present numerical results for this potential in Table IV. For all cases the singlet state has higher energy than the corresponding triplet state, except for pairs of odd parity. We can thus conclude that the *alternating rule* is followed by all presented states in the full potential.

As a limiting case for confinement with positive-power-law potentials we consider the planar hard-wall potential, which in modified units reads

$$V_{\text{billiard}}(\boldsymbol{r}) = \begin{cases} 0 & |\boldsymbol{r}| < 1, \\ \infty & |\boldsymbol{r}| \geqslant 1. \end{cases} \tag{21}$$

The radial solutions of the one-particle system are Bessel functions of the first kind,

$$\psi_{n,m}(r) = \mathcal{N}_{n,m}\, J_m\left(z(m,n+1)\, r\right), \tag{22}$$

where $z(m,n)$ is the nth zero of $J_m(r)$ and $\mathcal{N}_{n,m}$ is a properly defined normalization factor. The corresponding eigenenergies are given by $E_{n,m} = \frac{1}{2}[z(m,n+1)]^2$. The matrix elements,

$$_{\text{ind}}\langle |n_1,m_1,n_2,m_2| \frac{1}{|\boldsymbol{r}_1 - \boldsymbol{r}_2|} |n_1',m_1',n_2',m_2'\rangle_{\text{ind}}, \tag{23}$$

can be calculated via the multipole expansion of the Coulomb term. For each matrix element we calculate approximately 40 terms of the multipole expansion and estimate the remainder as described in Ref. [34]. With the equally symmetrized basis, as for the quartic potential case, Eq. (18), we evaluate the first- and second-order corrections. We consider all states for $m = 0$ from the ground state up to the quadruplet of states with degenerate unperturbed eigenenergy equal to $E = 102.935354$ m.u. (see Table V). We compare the energies for full Coulomb interaction ($\gamma = 1$). For mixed- and even-parity pairs singlet states are higher in energy than the corresponding triplet states, while for odd-parity pairs this behavior is reversed. Again, we can conclude, that all considered states follow the *alternating rule*.

VII. CONCLUSION

The extraordinary property of the harmonic confinement potential to be separable in COM and relative coordinates for any kind of interaction between the particles makes this model so simple and successful in the description of quantum dots. Recent investigations [16,21] consider the validity of the extension of HFR to excited states in a planar two-electron quantum dot model with harmonic confinement. For the application of HFR it is a necessary condition that the singlet and triplet states compared arise from symmetrization of the same one-electron orbitals. Our analysis shows, that in contrast to assumptions in these works, HFR rule is in general not applicable.

Entanglement witnesses in the noninteracting limit have revealed that the effect of the interaction is twofold. By the choice of a particular symmetry class the interaction induces entanglement for various states, already in the limit of vanishing interaction strength. Secondly, turning on the interaction further entangles the states as described in recent investigations [23,24,31]. The offset entanglement can be calculated for the noninteracting model solely by imposing the correct symmetrization of the state. As a consequence it can at least qualitatively explain several effects reported in the recent literature: (i) the nonvanishing entanglement in the noninteracting limit in harmonically confined two-electron quantum dot structures [24]; (ii) the different saturation limit for the entanglement in these models in comparison with helium [24,26]; (iii) the minimum in the linear entropy linked with the transition from cylindrical to spherical symmetry in the model involving a magnetic field [31]. For the last case it would be particularly interesting to investigate the entanglement for excited states. We expect the entanglement in the noninteracting limit to depend discontinuously on the magnetic field.

We have shown the concept of fermionic entanglement witnesses to be a proper tool to investigate the applicability of HFR. The entanglement witnesses were calculated analytically in the noninteracting system by choosing an appropriate basis. Only four states, arising from the degenerate levels of $E = 3$ m.u. for the noninteracting case can be compared at all. Analyzing these states, we found that the original explanation by Slater generally holds for these states. That is, the difference in the Coulombic interparticle interaction term is responsible for the higher energy of the singlet state. Furthermore, the angular momentum quantum number in relative coordinates is found to be the origin of the Fermi hole and has provided us with a deeper understanding of the difference in the interaction energy.

At first sight, the behavior for the quartic confinement potential appeared to be peculiar, since HFR is reversed for pairs of odd-parity states with zero angular momentum. Nevertheless it turns out that this behavior is the expected one, which was already well known for atomic systems [3]. For the lowest quadruplet of degenerate states in all four symmetry classes we have shown approximate quantum numbers in COM and relative coordinates to be a meaningful concept in order to understand the origin of the *alternating rule* in the quartic confinement potential. The localization of the wave functions is in agreement with the shape of the effective potentials according to the approximate quantum numbers. This is again the origin of the difference in the Coulomb interaction energy, which follows the same trend as the total energy in all considered cases.

First-order perturbation theory proved to give meaningful results for the harmonic and the quartic confining potentials considered in this work. Our results for the billiard case resemble those for the quartic confinement and the *alternating rule* is again valid, up to second-order perturbation theory.

The shell filling for few-electron quantum dots with a quartic potential perturbing the harmonic confinement has been considered in Ref. [20] and Hund's rules were found to be valid. This is true for the ground states of a quantum dot with a varying number of electrons. Nevertheless, in the two-electron case, the extended application of HFR to excited states holds only for even parity, while for odd parity the more general *alternating rule* needs to be applied and we have shown strong evidence that it is extensively valid.

The harmonic confinement seems to be the exception, where HFR is applicable for a minority of states only, while in other systems, lacking the separability in COM and relative coordinates, the applicability of HFR or the *alternating rule* is generally given. Furthermore, we believe that the *alternating*

rule, as an extension of HFR to pairs of odd-parity states, is valid for a wide range of confining potentials, as long as the correlation effects are to a certain extent weak. We have shown evidence that for small deviations from the harmonic confinement, which is a realistic assumption for the description of quantum dots, the *alternating rule* is valid. This might be confirmed experimentally by considering the energy splitting of odd-parity singlet and triplet states.

ACKNOWLEDGMENTS

The authors thank Tim-Oliver Müller and Martin Fink for fruitful discussions. S.S. is grateful for the support of the TU München graduate school.

APPENDIX A: MODIFIED UNITS

The Hamiltonian of two electrons of reduced mass m_* in a quantum dot reads

$$H = \sum_{j=1}^{2}\left[\frac{1}{2m_*}\tilde{\boldsymbol{p}}_j^2 + \tilde{V}_{\text{conf}}(\tilde{\boldsymbol{r}}_j)\right] + \frac{\tilde{\gamma}e^2}{4\pi\epsilon\epsilon_0|\tilde{\boldsymbol{r}}_1 - \tilde{\boldsymbol{r}}_2|}. \quad \text{(A1)}$$

Here, the Coulomb repulsion can be adiabatically tuned by the dimensionless Coulomb parameter $\tilde{\gamma}$ and it is affected by the dielectric properties of the confining system manifested through the dielectric constant ϵ. The confining potential is chosen to be one of

$$\tilde{V}_{\text{harmonic}}(\tilde{\boldsymbol{r}}) = \tfrac{1}{2}m_*\omega^2\tilde{\boldsymbol{r}}^2, \quad \text{(A2)}$$

$$\tilde{V}_{\text{quartic}}(\tilde{\boldsymbol{r}}) = \kappa(\tilde{\boldsymbol{r}}^2)^2, \quad \text{(A3)}$$

$$\tilde{V}_{\text{billiard}}(\tilde{\boldsymbol{r}}) = \begin{cases} 0 & \tilde{r} < R, \\ \infty & \tilde{r} \geqslant R. \end{cases} \quad \text{(A4)}$$

We introduce a natural length scale a_0 for each of these potentials:

$$a_0 = \sqrt{\frac{\hbar}{m_*\omega}}, \quad \text{(A5)}$$

$$a_0 = \sqrt[6]{\frac{\hbar^2}{m_*\kappa}}, \quad \text{(A6)}$$

$$a_0 = R, \quad \text{(A7)}$$

respectively. The natural energy scale is thus defined by $E_0 = \frac{\hbar^2}{m_* a_0^2}$. Rescaling (A1) with these modified units (m.u.) leads to the Hamiltonian (1). The following expression is obtained for the adiabatic Coulomb strength parameter:

$$\gamma = \frac{e^2 m_* a_0}{4\pi\epsilon\epsilon_0\hbar^2}\tilde{\gamma}. \quad \text{(A8)}$$

A typical harmonic confinement energy is $\hbar\omega \approx 3$meV [19] with the effective electron mass $m_* = 0.023\,m_e$ ($m_* = 0.063\,m_e$) and dielectric constant $\epsilon \approx 15.15$ ($\epsilon \approx 12.9$) for InAs (GaAs) semiconductor quantum dots. The natural length scale is $a_0 \approx 33$ nm ($a_0 \approx 20$ nm) and the Coulomb strength parameter is $\gamma \in [0,1]$ ($\gamma \in [0,1.9]$). We also use these values for the quartic and hard-wall potentials.

APPENDIX B: CALCULATION OF THE ENTANGLEMENT WITNESSES

To be able to perform the partial trace over one particle for the pure-state density matrix $|\psi\rangle\langle\psi| = |n_c,m_c,n_r,m_r\rangle^{\epsilon_p\,\epsilon_p}\langle n_c,m_c,n_r,m_r|$ we need to express this quantity in some independent particle basis. Thus, we transform to a basis associated with Cartesian coordinates $|C_x,C_y,R_x,R_y\rangle^{\epsilon_p} = |n_c,m_c,n_r,m_r\rangle^{\epsilon_p}$ with $n_c = \min(C_x,C_y)$, $m_c = |C_x - C_y|$, $n_r = \min(R_x,R_y)$, and $m_r = \pm|R_x - R_y|$ (such that $m_c + m_r = C_x - C_y + R_x - R_y$). The Cartesian basis in COM (C_x,C_y) and relative (R_x,R_y) coordinates is defined by

$$|C_x,C_y,R_x,R_y\rangle^{\epsilon_p} = \begin{cases} |C_x,C_y,R_x,R_y\rangle & \text{if } C_x = C_y \wedge R_x = R_y, \\ (|C_x,C_y,R_x,R_y\rangle + \epsilon_p|C_y,C_x,R_y,R_x\rangle)/\sqrt{2} & \text{otherwise.} \end{cases}$$

It is easy to evaluate the transformation into the Cartesian independent particle basis $|n_x,n_y,k_x,k_y\rangle$ making use of the simple harmonic oscillator operator algebra and a symmetric coordinate transformation. The transformation matrix elements are given by

$$\langle n_x,n_y,k_x,k_y|C_x,C_y,R_x,R_y\rangle = \sqrt{\frac{n_x!n_y!k_x!k_y!}{C_x!C_y!R_x!R_y!}}\sqrt{1/2}^{(n_x+n_y+k_x+k_y)}F(C_x,R_x,k_x)\delta_{C_x+R_x,n_x+k_x}F(C_y,R_y,k_y)\delta_{C_y+R_y,n_y+k_y}, \quad \text{(B1)}$$

with the function $F(N,M,k) := \sum_{r=\max(0,k-N)}^{\min(k,M)}\binom{N}{k-r}\binom{M}{k}(-1)^r$. With this we can write

$$\begin{aligned}|\psi\rangle\langle\psi| &= |n_c,m_c,n_r,m_r\rangle^{\epsilon_p\,\epsilon_p}\langle n_c,m_c,n_r,m_r| = |C_x,C_y,R_x,R_y\rangle^{\epsilon_p}\langle C_x,C_y,R_x,R_y|^{\epsilon_p} \\ &= \sum_{n_x,n_y,k_x,k_y,\tilde{n}_x,\tilde{n}_y,\tilde{k}_x,\tilde{k}_y} |n_x,n_y,k_x,k_y\rangle\langle n_x,n_y,k_x,k_y|C_x,C_y,R_x,R_y\rangle^{\epsilon_p\,\epsilon_p}\langle C_x,C_y,R_x,R_y|\tilde{n}_x,\tilde{n}_y,\tilde{k}_x,\tilde{k}_y\rangle\langle\tilde{n}_x,\tilde{n}_y,\tilde{k}_x,\tilde{k}_y|.\end{aligned}$$

The trace over one of the particles can now be performed easily.

[1] F. Hund, Z. Phys. **33**, 345 (1925).
[2] F. Hund, Z. Phys. **34**, 296 (1925).
[3] J. D. Morgan and W. Kutzelnigg, J. Phys. Chem. **97**, 2425 (1993).
[4] J. C. Slater, Phys. Rev. **34**, 1293 (1929).
[5] E. R. Davidson, J. Chem. Phys. **42**, 4199 (1965).
[6] Y. Accad, C. L. Pekeris, and B. Schiff, Phys. Rev. A **4**, 516 (1971).
[7] E. A. Colbourn and C. A. Coulson, J. Phys. B: At. Mol. Opt. **7**, 1574 (1974).
[8] R. J. Boyd and C. A. Coulson, J. Phys. B: At. Mol. Opt. **6**, 782 (1973).
[9] D. A. Kohl, J. Chem. Phys. **56**, 4236 (1972).
[10] H. Tatewaki and K. Tanaka, J. Chem. Phys. **60**, 601 (1974).
[11] J. Colpa and M. Islip, Mol. Phys. **25**, 701 (1973).
[12] J. Colpa, A. J. Thakkar, V. H. Smith, and P. Randle, Mol. Phys. **29**, 1861 (1975).
[13] R. J. Boyd, Nature (London) **310**, 480 (1984).
[14] Y. Sajeev, M. Sindelka, and N. Moiseyev, J. Chem. Phys. **128**, 061101 (2008).
[15] W. Kutzelnigg and I. Morgan J. D., Z. Phys. D **36**, 197 (1996).
[16] T. Sako, J. Paldus, A. Ichimura, and G. H. F. Diercksen, J. Phys. B: At. Mol. Opt. **45**, 235001 (2012).
[17] J. Katriel and S. I. Themelis, Int. J. Quantum Chem. **112**, 2880 (2012).
[18] S. Tarucha, D. G. Austing, T. Honda, R. J. van der Hage, and L. P. Kouwenhoven, Phys. Rev. Lett. **77**, 3613 (1996).
[19] L. P. Kouwenhoven, D. G. Austing, and S. Tarucha, Rep. Prog. Phys. **64**, 701 (2001).
[20] P. Matagne, J. P. Leburton, D. G. Austing, and S. Tarucha, Phys. Rev. B **65**, 085325 (2002).
[21] T. Sako, J. Paldus, and G. H. F. Diercksen, Phys. Rev. A **81**, 022501 (2010).
[22] A. R. Plastino, D. Manzano, and J. S. Dehesa, Europhys. Lett. **86**, 20005 (2009).
[23] D. Manzano, A. R. Plastino, J. S. Dehesa, and T. Koga, J. Phys. A: Math. Gen. **43**, 275301 (2010).
[24] A. P. Majtey, A. R. Plastino, and J. S. Dehesa, J. Phys. A: Math. Gen. **45**, 115309 (2012).
[25] J. S. Dehesa, T. Koga, R. J. Yáñez, A. R. Plastino, and R. O. Esquivel, J. Phys. B: At. Mol. Opt. **45**, 015504 (2012).
[26] Y.-C. Lin, C.-Y. Lin, and Y. K. Ho, Phys. Rev. A **87**, 022316 (2013).
[27] S. Schröter, P.-A. Hervieux, G. Manfredi, J. Eiglsperger, and J. Madroñero, Phys. Rev. B **87**, 155413 (2013).
[28] T. Oyamada, K. Hongo, Y. Kawazoe, and H. Yasuhara, J. Chem. Phys. **133**, 164113 (2010).
[29] G. Ghirardi, L. Marinatto, and T. Weber, J. Stat. Phys. **108**, 49 (2002).
[30] G. C. Ghirardi and L. Marinatto, Phys. Rev. A **70**, 012109 (2004).
[31] R. G. Nazmitdinov, N. S. Simonović, A. R. Plastino, and A. V. Chizhov, J. Phys. B: At. Mol. Opt. **45**, 205503 (2012).
[32] R. G. Nazmitdinov, N. S. Simonović, and J. M. Rost, Phys. Rev. B **65**, 155307 (2002).
[33] S. Bell, R. Davidson, and P. A. Warsop, J. Phys. B: At. Mol. Opt. **3**, 113 (1970).
[34] S. Sawada, A. Terai, and K. Nakamura, Chaos Solitons Fractals **40**, 862 (2009).